

# The 2-3 mixing and mass split: atmospheric neutrinos and magnetized spectrometers

Abhijit Samanta<sup>a,b</sup> and A. Yu. Smirnov<sup>b</sup>

<sup>a</sup>*Ramakrishna Mission Vivekananda University, Belur Math, Howrah 711 202, India*

<sup>b</sup>*The Abdus Salam International Centre for Theoretical Physics  
Strada Costiera 11, I-34014 Trieste, Italy*

We study dependence of the atmospheric  $\nu_\mu$  and  $\bar{\nu}_\mu$  fluxes on the deviations of 2-3 mixing from maximal  $|45^\circ - \theta_{23}|$ , on the  $\theta_{23}$ -octant and on the neutrino mass split  $\Delta m_{32}^2$ . Analytic expressions for the effect of  $\theta_{23}$  deviation and the octant asymmetry are derived. We present conservative estimations of sensitivities of iron (magnetized) calorimeter detectors (ICAL) to these parameters. ICAL can establish the  $\theta_{23}$ -deviation at  $3\sigma$  confidence level if  $|45^\circ - \theta_{23}| > 6^\circ$  with exposure of 1 Mton-yr. Sensitivity to the octant is low for zero or very small 1-3 mixing, but it can be substantially enhanced for  $\theta_{13} > 3^\circ$ . ICAL can measure the difference of  $\Delta m_{32}^2$  in  $\nu$  and  $\bar{\nu}$  channels (CPT test) with accuracy  $0.8 \times 10^{-4} \text{ eV}^2$  at  $3\sigma$  confidence level with 1 Mton-yr exposure and the present MINOS result can be excluded at  $> 5\sigma$  confidence level. We discuss possible ways to further improve the sensitivity of magnetized spectrometers.

PACS numbers: 14.60.Pq, 14.60.Lm

## I. INTRODUCTION

Determination of the 2-3 mass split and leptonic mixing, and in particular, its deviation from the maximal mixing:

$$\delta_{23} \equiv 45^\circ - \theta_{23} \quad (1)$$

is of the fundamental importance<sup>1</sup>. Here we use the standard parameterization of the PMNS mixing matrix:

$$U_{PMNS} = U_{23}(\theta_{23})\Gamma_\delta U_{13}(\theta_{13})U_{12}(\theta_{12}), \quad (2)$$

where  $U_{ij}$  are matrices of rotation in  $ij$  plane. Being maximal or close to maximal, the 2-3 mixing testifies for existence of certain underlying symmetry [1]. Comparison of values of  $\delta_{23}$  and  $\theta_{13}$  as well as mixing angles of quarks can shed some light on the origins of fermion mass and mixing in general.

The existing results on determination of  $\theta_{23}$  and  $\Delta m_{32}^2$  are summarized in the Table 1. Note that the global fit of oscillation data [2] (see also [3]) show some deviation of 2-3 mixing from maximal:  $\delta_{23} = 2 - 3^\circ$  ( $1\sigma$ ). Although the data agree well with maximal mixing, large deviation  $\delta_{23} = \pm 9^\circ$  ( $3\sigma$ ) is still possible.

Concerning the 2-3 mass split, the global fit results are also in agreement with result of SK [4] and result of MINOS measurement in the  $\nu$  channel [5].

Recently MINOS has reported the values of  $\Delta m_{31}^2$  and  $\theta_{23}$  in  $\bar{\nu}$  channel [5] which differ from those in  $\nu$  channel (see tables I and II). If confirmed, this result will testify for an effective, (due to existence of some new interactions [6]) or fundamental CPT violation. The analysis of the atmospheric neutrino data does not confirm MINOS result although the sensitivity of SK to CPT violation effects is not high since SK sum up the interactions of neutrinos and antineutrinos [6]. ICAL can perform very sensitive for the CPT violation and check MINOS result.

New accelerator experiments T2K and NO $\nu$ A will improve precision of measurements of  $\Delta m_{32}^2$  by factor 2, but their accuracy of measurements of  $\theta_{23}$  will be only slightly better than that of present global fit (see table I).

There are two aspects of the  $\theta_{23}$ -determination:

- measurement of the absolute value of deviation:  $|\delta_{23}|$ ;
- identification of the  $\theta_{23}$ -octant, *i.e.* the sign of  $\delta_{23}$  or resolution of the octant degeneracy.

The problem of determination of  $\delta_{23}$  and the octant with atmospheric neutrinos has been addressed in a number of publications before [8–14]. It was realized [9–11] that at low energies the oscillation effects on the electron neutrino flux are proportional to this deviation, and therefore searches for an excess (or suppression) of events in the sub-GeV range would testify for  $\delta_{23}$ .

For water Cherenkov detectors the above two aspects of 2-3 mixing have been explored in [10, 11]. The study has been mainly concentrated on effects in the electron neutrino flux.

<sup>1</sup>  $\delta_{23}$  is related to another used deviation parameter,  $D_{23} \equiv 1/2 - \sin^2 \theta_{23}$ , as  $D_{23} = \sin 2\delta_{23}$ .

A magnetized calorimeters can only detect muon neutrinos, but it can distinguish neutrinos and antineutrinos which compose its main advantage. These detectors provide better energy and angle resolution of charge leptons, and consequently, neutrinos. A possibility to disentangle neutrinos and antineutrinos reinforces the following features: i) energy and angular resolutions (reconstruction) are different for neutrinos and antineutrinos. ii) The sensitivity of neutrino and antineutrino channels to oscillation parameters is substantially different.

Sensitivity of a magnetized calorimeter to the 2-3 mixing and mass split has been explored in [12] and [13]. It has been found that the octant discrimination from high energy neutrinos at the nonzero 1-3 mixing is more feasible with the magnetized detector than with water Cherenkov detectors since the former can directly measure the matter effect [12]. In these studies, however, various simplifications have been made which do not allow for realistic estimations of potential of the experiments. In the analysis [15] the octant discrimination possibility has been evaluated for two benchmark values of  $\theta_{23}$  with a relatively high  $\theta_{13} = 7.5^\circ$ .

Here we present a comprehensive study of sensitivities of the ICAL to the parameters of the 2-3 sector. We assume that by the time of realization of this detector certain information about  $\theta_{13}$  will be obtained.

The paper is organized as follows. In sec. II we study dependence of the  $\nu_\mu$  and  $\bar{\nu}_\mu$  fluxes on parameters of the 2-3 sector:  $|\delta_{23}|$ , octant and  $\Delta m_{23}^2$ . In sec. III we describe details of our statistical analysis. We evaluate physics potential of the magnetized calorimeters to measure these parameters in sec. IV. Discussion and conclusions are given in sec. V. In sec. V we discuss possibilities of further improvements of sensitivities of magnetized calorimeters.

## II. DEPENDENCE OF THE ATMOSPHERIC NEUTRINO FLUXES ON 2-3 MIXING

The original atmospheric neutrino flux contains both the muon,  $F_\mu^0$ , and electron,  $F_e^0$ , neutrino components, so that the muon neutrino flux at a detector equals

$$\begin{aligned} F_\mu &= F_\mu^0 P_{\nu_\mu \rightarrow \nu_\mu} + F_e^0 P_{\nu_e \rightarrow \nu_\mu} \\ &= F_\mu^0 \left[ P_{\nu_\mu \rightarrow \nu_\mu} + \frac{1}{r} P_{\nu_e \rightarrow \nu_\mu} \right]. \end{aligned} \quad (3)$$

Here the flavor ratio

$$r(E, \theta_Z) \equiv \frac{F_\mu^0(E, \theta_Z)}{F_e^0(E, \theta_Z)} \quad (4)$$

is function of the neutrino energy  $E$  and zenith angle  $\theta_Z$ .

For the standard parameterization of the mixing matrix a dependence of the oscillation probabilities on the 2-3 mixing  $\theta_{23}$  and CP-phase  $\delta$  is *explicit* for an arbitrary density profile. This result follows from the order of rotation in eq. (2) and the fact that the matrix of matter potentials has the form  $V = \text{diag}\{V_e, 0, 0\}$  in the flavor basis, *i.e.* it is invariant under 2-3 rotations. Indeed, the neutrino evolution can be considered in the propagation basis,  $\tilde{\nu} \equiv (\nu_e, \tilde{\nu}_2, \tilde{\nu}_3)$ , defined via the following relation with the flavor basis:  $\nu_f \equiv U_{23} \Gamma_\delta \tilde{\nu}$ . Consequently,  $\tilde{\nu} = U_{13} U_{12} \nu_{\text{mass}}$ , where  $\nu_{\text{mass}} \equiv (\nu_1, \nu_2, \nu_3)$  is the basis of mass eigenstates. In the propagation basis the Hamiltonian, and therefore, the amplitudes of transitions depend on  $\theta_{13}, \theta_{12}, V_e$ , and mass squared differences:

$$A_{\alpha\beta} = A_{\nu_\alpha \rightarrow \nu_\beta}(\theta_{13}, \theta_{12}, V_e), \quad \alpha, \beta = e, \tilde{2}, \tilde{3}, \quad (5)$$

and they do not depend on  $\theta_{23}$  and  $\delta$ . In the flavor basis the dependence of the amplitudes on these parameters appears via projections from the propagation basis to the flavor basis:

$$\hat{A}^f = U_{23} \Gamma_\delta \hat{A} \Gamma_{-\delta} U_{23}^T, \quad (6)$$

where  $\hat{A}^f$  and  $\hat{A}$  are the corresponding matrices of amplitudes.

In terms of the propagation basis amplitudes  $A_{\alpha\beta}$  one can rewrite the muon flux eq. (3) in the following form [16]:

$$\begin{aligned} \frac{F_\mu}{F_\mu^0} &\approx 1 - \frac{1}{2} \sin^2 2\theta_{23} \sin^2 \frac{\phi_{23}}{2} \\ &- \frac{1}{2} \sin^2 2\theta_{23} \cos \phi_{23} [1 - \text{Re}(A_{2\tilde{2}}^* A_{3\tilde{3}})] \\ &- \left( s_{23}^4 - \frac{s_{23}^2}{r} \right) P_A - \left( c_{23}^4 - \frac{c_{23}^2}{r} \right) P_S \\ &- \sin 2\theta_{23} P_\delta, \end{aligned} \quad (7)$$

where

$$\tilde{P}_A \equiv |A_{e\tilde{3}}|^2, \quad \tilde{P}_S \equiv |A_{e\tilde{2}}|^2, \quad (8)$$

are the probabilities of transitions  $\nu_e \rightarrow \tilde{\nu}_2$  and  $\nu_e \rightarrow \tilde{\nu}_3$  correspondingly, and  $P_\delta$  is the function which depends on the CP-violation phase. In eq. (7)  $\phi$  is the oscillation phase due to the 2-3 mass split,  $c_{23} \equiv \cos^2 \theta_{23}$ , *etc.*. Notice that  $\tilde{P}_S, \tilde{P}_A, P_\delta$  and  $\phi$  do not depend on  $\theta_{23}$ .

In eq. (7) the first two terms are due to vacuum oscillations driven by the 2-3 mixing and mass split; the second line is an interference of the 2-3 and 1-2 modes of oscillations. The product of amplitudes in this term can be approximated as

$$|A_{\bar{2}\bar{2}}A_{\bar{3}\bar{3}}| \approx \sqrt{(1 - \tilde{P}_A)(1 - \tilde{P}_S)}. \quad (9)$$

The terms in the third line describe effects of oscillations due to the 1-2 and 1-3 mixing. The last term describes the CP-violation. The leading (second) term as well as the interference and CP-violating terms are symmetric with respect change of sign of the deviation:  $\delta_{23} \rightarrow -\delta_{23}$ . The octant symmetry (degeneracy) is broken by terms in the third line which vanish for maximal mixing and  $r = 2$ .

For antineutrinos one gets the same formula eq. (7) with substitution  $\tilde{P}_S \rightarrow \tilde{\bar{P}}_S$ ,  $\tilde{P}_A \rightarrow \tilde{\bar{P}}_A$  and  $r \rightarrow \bar{r}$ .

The octant effect can be characterized by the octant asymmetry defined as

$$\frac{\Delta^{oct} F_\mu}{F_\mu^0} \equiv \frac{1}{F_\mu^0} [F_\mu(45^\circ + \delta_{23}) - F_\mu(45^\circ - \delta_{23})]. \quad (10)$$

For such symmetric deviations from maximal mixing one has

$$\begin{aligned} \Delta(\sin^2 2\theta_{23}) &= 0, \\ \Delta(\cos^2 \theta_{23}) &= \Delta(\cos^4 \theta_{23}) = -\sin 2\delta_{23}. \end{aligned} \quad (11)$$

Then according to eq. (7) the octant asymmetry equals

$$\frac{\Delta^{oct} F_\mu}{F_\mu^0} = \sin 2\delta_{23} \left(1 - \frac{1}{r}\right) (\tilde{P}_S - \tilde{P}_A). \quad (12)$$

Notice that  $\tilde{P}_S$  and  $\tilde{P}_A$  enter the asymmetry with opposite signs and therefore partly cancel each other. To get an idea about dependences of the probabilities on the neutrino parameters one can use expressions for the amplitudes in medium with constant density:

$$\begin{aligned} A_{e\bar{2}} &= c_{13}^m \sin 2\theta_{12}^m \sin \phi_{21}^m, \\ A_{e\bar{3}} &= \sin 2\theta_{13}^m \\ &\times \left( \sin \phi_{32}^m e^{-i\phi_{31}^m} + \cos^2 \theta_{12}^m \sin \phi_{21}^m \right). \end{aligned} \quad (13)$$

The probability  $\tilde{P}_S \propto \sin^2 2\theta_{12}^m$  decreases with energy, whereas  $\tilde{P}_A \propto \sin^2 2\theta_{13}^m$  increases being resonantly enhanced in the neutrino channel (for normal mass hierarchy) at high energies. Here sensitivity of ICAL to the sign of the charge of muon plays certain role. The two probabilities become comparable at 1 GeV for  $\sin^2 \theta_{13} \sim 0.01$ .

In the limit of zero 1-3 mixing one finds from eq. (7)

$$\begin{aligned} \frac{F_\mu}{F_\mu^0} &\approx 1 - \sin^2 2\theta_{23} \sin^2 \frac{\phi}{2} - \frac{1}{2} \sin^2 2\theta_{23} \\ &\times \left(1 - \sqrt{1 - P_S}\right) \cos \phi - \left(c_{23}^4 - \frac{c_{23}^2}{r}\right) P_S, \end{aligned} \quad (14)$$

where  $P_S = \tilde{P}_S(\theta_{13} = 0)$ , which is the  $2\nu$  probability of oscillations driven by  $\Delta m_{21}^2$  and  $\theta_{12}$ . For the octant asymmetry we obtain

$$\frac{\Delta^{oct} F_\mu}{F_\mu^0} = \sin 2\delta_{23} \left(1 - \frac{1}{r}\right) P_S. \quad (15)$$

At low energies:  $r \approx 2$ , and therefore the asymmetry equals  $\sim 1/2 \sin 2\delta_{23} P_S$ .

In fig. 1 we show the oscillograms for the octant asymmetry, lines of equal asymmetry  $\Delta^{oct} F_\mu / F_\mu^0$  in the  $E - \cos \theta_Z$  plane in neutrino and antineutrino channels. According to eq. (15) these oscillograms coincide with the oscillograms for  $P_S$  up to coefficient which weakly depends on  $E$  and  $\theta_Z$  at  $E < 1$  GeV. We use  $\delta_{23} = 5^\circ$ ,  $\theta_{13} = 0$ , and other parameters are set at their best-fit values. The asymmetry increases with decrease of neutrino energy. Maximal asymmetry is achieved in the 1-2 resonance ( $E \sim 0.1$  GeV):  $\Delta^{oct} F_\mu / F_\mu^0 \approx 0.087$ . For realistic threshold  $E_{th} = 0.3$  GeV and  $\delta_{23} = 5^\circ$  the averaged asymmetry is about (2 - 3)% and for  $E_{th} = 0.8$  GeV it is below 1%.

Notice that the octant asymmetry is about 4 times stronger for the electron neutrinos:

$$\frac{\Delta^{oct} F_e}{F_e^0} = -\sin 2\delta_{23} r P_S. \quad (16)$$

Here, however, the original flux is 2 times smaller. Furthermore, detection of muons provide better energy and direction resolutions.

Since  $P_S$  and  $\bar{P}_S$  are of the same order, a separation of the neutrino and antineutrino signals has no sense here.

Let us consider variations of the  $\nu_\mu$ -flux due to the  $\theta_{23}$ -deviation from maximal mixing. According to (7) the relative change of the flux equals

$$\begin{aligned} \frac{\Delta^{dev} F_\mu}{F_\mu^0} &\equiv \frac{F_\mu(45^\circ) - F_\mu(45^\circ - \delta_{23})}{F_\mu^0} \\ &\approx -\frac{1}{2} \Delta(\sin^2 2\theta_{23}) \sin^2 \frac{\phi_{23}}{2} \\ &\cong -\frac{1}{2} \sin^2 2\delta_{23}, \end{aligned} \quad (17)$$

where in the last equality we have averaged the oscillations due to large mass split.

Ratio of octant asymmetry and deviation effect equals

$$\frac{\Delta^{oct} F_\mu}{\Delta^{dev} F_\mu} = -\frac{1}{\sin 2\delta_{23}} \left(1 - \frac{1}{r}\right) (\langle \tilde{P}_S \rangle - \langle \tilde{P}_A \rangle), \quad (18)$$

where  $\langle \tilde{P}_S \rangle$  and  $\langle \tilde{P}_A \rangle$  are the probabilities averaged over the experimental  $E - \cos \theta_Z$  ranges. Although  $\Delta^{dev} F_\mu^0$  is proportional to square of the deviation parameter, for not very small  $\delta_{23}$  ( $> 5^\circ$ ) and  $\theta_{13} = 0$ , the integral effect of the deviation from maximal mixing is stronger than the effect of octant. The reason is that the deviation effect does not change with energy, whereas the octant asymmetry being proportional to  $P_S$  quickly decreases with  $E$  ( $\langle \tilde{P}_S \rangle \ll \langle \tilde{P}_A \rangle$ ). For zero 1-3 mixing and  $\delta_{23} = 5^\circ$  we have  $\Delta^{dev} F_\mu / F_\mu^0 = 0.015$ , and  $\Delta^{oct} F_\mu / F_\mu^0 = 0.087 \langle P_S \rangle$ .

For non-zero 1-3 mixing at high energies the ratio of the flux differences is

$$\frac{\Delta^{oct} F_\mu}{\Delta^{dev} F_\mu} \cong \left(1 - \frac{1}{r}\right) \frac{\langle \tilde{P}_A \rangle}{\sin 2\delta_{23}}, \quad (19)$$

and since  $P_A$  does not decrease with energy the ratio is not small.

We will use the considerations of this section for interpretation of numerical results. In our studies of sensitivities we obtain the oscillation probabilities solving numerically full three flavor evolution equation and using the Preliminary Reference Earth Model (PREM) [17] for the density profile of the Earth.

### III. THE $\chi^2$ ANALYSIS FOR ICAL

To evaluate physics potential of the atmospheric neutrino studies with the magnetized ICAL detector we generated atmospheric neutrino events and considered the muon energy and direction (directly measurable quantities) using event generator NUANCE-v3 [18]. The GEANT [19] simulation of ICAL detector shows that the energy and angular resolutions of the muons are very high and the corresponding uncertainties are negligible compared to the angle and energy uncertainties (changes) of the scattering processes.

$\chi^2$  is calculated according to the Poisson distribution. The term due to the contribution of prior information on the oscillation parameters measured by other experiments is not added to  $\chi^2$  for conservative estimation. The data have been binned in cells of equal size in the  $\log_{10} E - L^{0.4}$  plane, where  $L = 2R \cos \theta_Z$ . Choice of this binning is motivated by pattern of the oscillation probability  $P(\nu_\mu \rightarrow \nu_\mu)$  in

the  $L - E$  plane [20]. The distance between two consecutive oscillation peaks increases (decreases) as one goes to lower  $L$  ( $E$ ) values for a given  $E$  ( $L$ ). The binning of  $L$  has been optimized to get better sensitivity to oscillation parameters. To maintain  $\chi^2/d.o.f \approx 1$  in Monte Carlo simulation study, number of events should be  $> 4$  per cell [15]. If the number is smaller than 4 (which happens in the high energy bins), we combine results from the nearest cells.

For each set of oscillation parameters we integrate the atmospheric neutrino flux at the detector over the energy and zenith angle folding it with the cross section, the exposure time, the target mass, the efficiency of detection and the two dimensional energy-angle correlated resolution functions to obtain the data for the  $\chi^2$  analysis. We use the charge current cross section of NUANCE-v3 [18] and the Honda flux in the 3-dimensional scheme [21].

The systematic uncertainties of the atmospheric neutrino flux are crucial for determination of the oscillation parameters. We have divided them into two categories: (i) the overall flux normalization uncertainties which are independent of the energy and zenith angle, and (ii) the spectral tilt uncertainties which depend on  $E$  and  $\theta_Z$ .

The flux with uncertainties included can be written as

$$\Phi(E, \theta_Z) = \Phi_0(E) \left[1 + \delta_E \log_{10} \frac{E}{E_0}\right] \times [1 + \delta_Z (|\cos \theta_Z| - 0.5)] \times [1 + \delta_{f_N}]$$

For  $E < 1$  GeV we take the energy dependent uncertainty  $\delta_E = 15\%$  and  $E_0 = 1$  GeV and for  $E > 10$  GeV,  $\delta_E = 5\%$  and  $E_0 = 10$  GeV. The overall flux uncertainty as a function of zenith angle is parameterized by  $\delta_Z$ . According to [21] we use  $\delta_Z = 4\%$  which leads to 2% vertical/horizontal flux uncertainty. We take for the overall flux normalization uncertainty  $\delta_{f_N} = 10\%$  and for the overall neutrino cross-section uncertainty  $\delta_\sigma = 10\%$ .

In our  $\chi^2$  analysis the numbers of events have been computed for the theoretical (fit values) and experimental (true) values of parameters in the same way by migrating number of events from neutrino to muon energy and zenith angle bins. The resolution functions have been taken from the previous work [22].

In studies of sensitivity to the 2-3 mixing we marginalize  $\chi^2$  over  $\Delta m_{32}^2$ ,  $\theta_{13}$ ,  $\delta_{CP}$  for  $\nu$ 's and  $\bar{\nu}$ 's separately. Then we find the total  $\chi^2$  as  $\chi^2 = \chi_\nu^2 + \chi_{\bar{\nu}}^2$ . We have chosen the following bench mark values of neutrino parameters for this analysis:  $\Delta m_{32}^2 = 2.5 \times 10^{-3}$  eV<sup>2</sup>,  $\delta_{CP} = 0$ ,  $\Delta m_{21}^2 = 7.9 \times 10^{-5}$  eV<sup>2</sup> and  $\theta_{12} = 34.24^\circ$ . In marginalization we use flat dis-

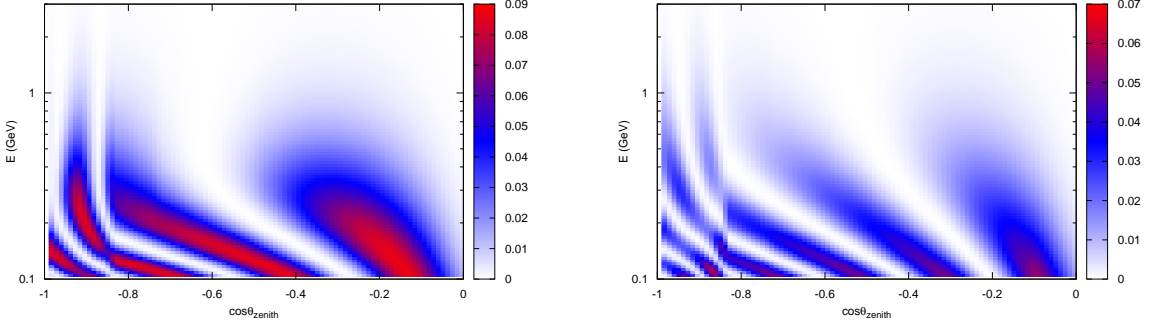


FIG. 1: The oscillogram for the octant asymmetry  $\frac{\Delta^{oct} F_\mu}{F_\mu^0}$  for neutrino (left) and antineutrino (right) with  $\delta_{23} = 5^\circ$  at  $\theta_{13} = 0$ . The other parameters are set at their best-fit values.

tributions of values of the parameters in the following ranges:  $\Delta m_{32}^2 = (2.3-2.7) \times 10^{-3} \text{eV}^2$ ,  $\theta_{23} = 36^\circ - 54^\circ$  and  $\theta_{13} = 0^\circ - 10.5^\circ$ . The range of  $\theta_{13}$  is changed for some particular analyses.

The parameters  $\Delta m_{21}^2$  and  $\theta_{12}$  produce sub-leading effects on atmospheric neutrino fluxes when  $E > \text{GeV}$ . Moreover, effect of these parameters in marginalization is very small due to narrow allowed regions. Therefore we have taken fixed values of  $\Delta m_{21}^2$  and  $\theta_{12}$  in our analysis.

#### IV. SENSITIVITIES OF ICAL

In our computations we used the neutrino energy range (0.141 -15) GeV with different thresholds and different exposures,  $\mathcal{E}$ , of 0.25, 1, 2, and 4 Mton-yr.

##### A. Determination of 2-3 mixing for $\theta_{13} = 0$

The sensitivity of ICAL experiment to  $\theta_{23}$  is shown in fig. 2. We plot  $\Delta\chi^2$  defined by

$$\Delta\chi^2 = \chi^2(\theta_{23}) - \chi^2(\theta_{23}^{true}) \quad (20)$$

as function of the fit value for fixed input values  $\theta_{23}^{true} = 37^\circ$ , (left) and  $40^\circ$  (right) with  $\mathcal{E} = 1, 2$ , and 4 Mton-yr. We have marginalized the  $\chi^2$  with respect to all oscillation parameters except  $\theta_{23}$ . The figures show high sensitivity to the deviation  $\delta_{23}$ : it would be possible to discriminate between a given  $\theta_{23}$  and maximal mixing at 99% CL if  $|\delta_{23}| > 5^\circ$ . For instance, after 1 Mton-yr the angle  $\theta_{23} = 37^\circ$  can be distinguished from  $45^\circ$  at 8 $\sigma$  level.

The figures show some sensitivity to the octant:  $\Delta\chi^2$  is higher in the right minima which correspond to wrong octant. However, the difference is small: After 1 Mton-yr exposure the difference of  $\Delta\chi^2$  in the true and wrong octants is smaller than 1. The difference becomes more than 2 (90% CL) only after 4 Mton-yr. Identification of the octant becomes even more difficult for smaller  $\delta_{23}$ . If  $\delta_{23} = 5^\circ$ , we find  $\Delta\chi^2 = 1.2$  after 4 Mton-yr. This result can be readily seen from our analytical consideration in sec. II. The probability  $P_S$  averaged over the energy interval (0.14 – 15) GeV equals  $\langle P_S \rangle \sim 0.02$ , so that for  $\delta_{23} = 8^\circ$ :  $\Delta^{oct} F_\mu / F_\mu^0 \sim 4 \cdot 10^{-3}$ , whereas  $\Delta^{dev} F_\mu / F_\mu^0 \sim 0.04$  - an order of magnitude larger. As we mentioned before, this big difference of sensitivities to the deviation and octant (degeneracy) is because the octant asymmetry is collected only at very low energies where  $P_S$  is unsuppressed, whereas whole energy range contributes to the sensitivity to the deviation.

The sensitivity drops down substantially with the deviation: Reducing  $\delta_{23}$  from  $8^\circ$  to  $5^\circ$  (compare the left and right panel of fig. 2) leads to decrease of the flux difference by factor 2.5, and correspondingly, significance of discrimination from maximal mixing becomes 2 $\sigma$  (for 1 Mton-yr) (right panel of fig. 2). Sensitivity to the octant at 1 $\sigma$  level appears only with 4 Mton-yr exposure.

In fig. 3 we have plotted the marginalized  $\Delta\chi^2$ , calculated at the maximal mixing (fit value) for different input (true) values of  $\theta_{23}$ :

$$\Delta^{dev} \chi^2 = \chi^2(45^\circ) - \chi^2(\theta_{23}^{true}). \quad (21)$$

The picture is complementary to that in fig. 2, and there is an approximate symmetry with respect to  $\theta_{23} = 45^\circ$ . The reason of sharp increase of  $\Delta\chi^2$  at 42 and 48 $^\circ$  is related to the dependence of oscillation



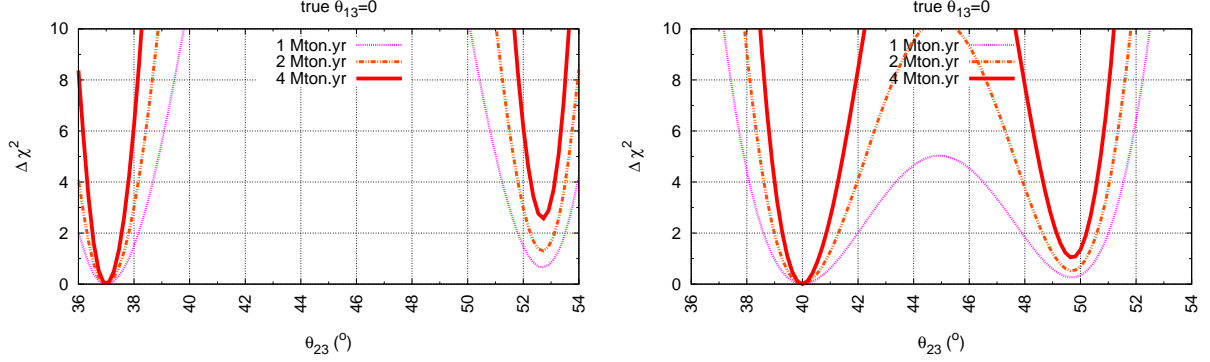


FIG. 2: The variation of the  $\Delta\chi^2$  with  $\theta_{23}$  for  $\theta_{13} = 0$  and for fixed input values of  $\theta_{23} = 37^\circ$  (left) and  $40^\circ$  (right) with  $\mathcal{E} = 1, 2$ , and  $4$  Mton-yr, respectively and threshold  $0.141$  GeV. The  $\chi^2$  is marginalized with respect to all oscillation parameters except  $\theta_{23}$ . The range of marginalization for  $\theta_{13}$  is  $0 - 10.5^\circ$ .

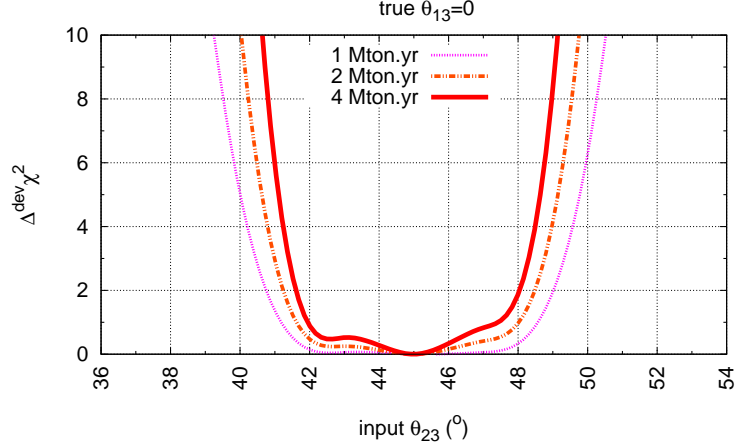


FIG. 3: The variation of the sensitivity to deviation from maximal mixing with different input values of  $\theta_{23}$  for  $\mathcal{E} = 1, 2$ , and  $4$  Mton-yr, respectively, and threshold  $0.141$  GeV. Here  $\Delta^{dev}\chi^2 = \chi^2(45^\circ) - \chi^2(\theta_{23}^{true})$ . The  $\chi^2$  is marginalized with respect to all oscillation parameters except  $\theta_{23}$ . The range of marginalization for  $\theta_{13}$  is  $0 - 10.5^\circ$ .

probability around  $\delta_{23} = 0$  and to overall flux uncertainty.

In fig. 4 we show dependence of sensitivity to the octant on  $\theta_{23}$ . For different input (true) values of  $\theta_{23}$  we plotted

$$\Delta^{oct}\chi^2 = \chi^2(90^\circ - \theta_{23}) - \chi^2(\theta_{23}). \quad (22)$$

According to fig. 4, it will be possible to discriminate the octant at 90% CL if  $\theta_{23} \lesssim 38^\circ$  or  $\gtrsim 52^\circ$  after  $\mathcal{E} = 4$  Mton-yr. Notice that the curves are nearly symmetric with respect to  $\theta_{23} = 45^\circ$ .

In fig. 5, we show the dependence of sensitivity to the octant on the energy threshold. Due to fast

decrease of  $P_S$  with increase of energy (see fig 1) the sensitivity disappears for high thresholds.

## B. Determination of $\theta_{23}$ in the presence of non-zero 1-3 mixing.

Analysis of oscillation data testifies for non-zero 1-3 mixing although significance is not high and zero value is not yet excluded. The global fit at  $1\sigma$  CL gives  $\theta_{13} = 7.3^\circ +2.1^\circ_{-3.2^\circ}$ , with  $3\sigma$  upper bound of  $\theta_{13} < 13^\circ$ , and  $\delta_{CP} \in [0, 360]$  [2]. Analysis of the solar and KAMLAND data by SNO collaboration leads

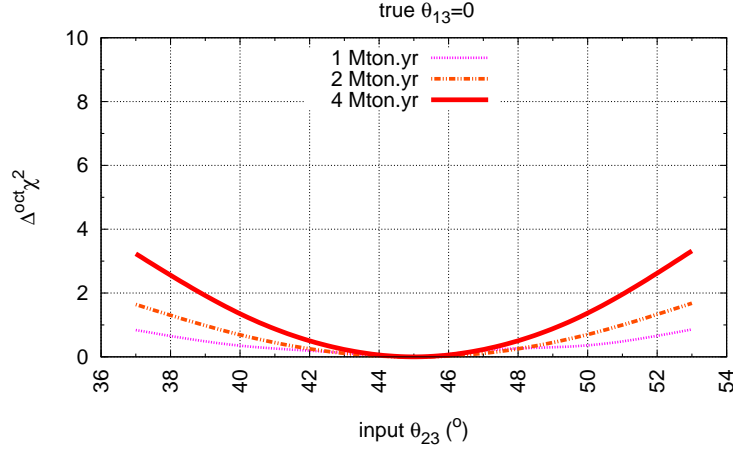


FIG. 4: The variation of the sensitivity to  $\theta_{23}$ -octant with different input values of  $\theta_{23}$  for  $\mathcal{E} = 1, 2$ , and 4 Mton·yr, respectively, and threshold 0.141 GeV. Here  $\Delta^{oct} \chi^2 = \chi^2(90^\circ - \theta_{23}) - \chi^2(\theta_{23})$ . The  $\chi^2$  is marginalized with respect to all oscillation parameters except  $\theta_{23}$ . The range of marginalization for  $\theta_{13}$  is  $0 - 10.5^\circ$ .

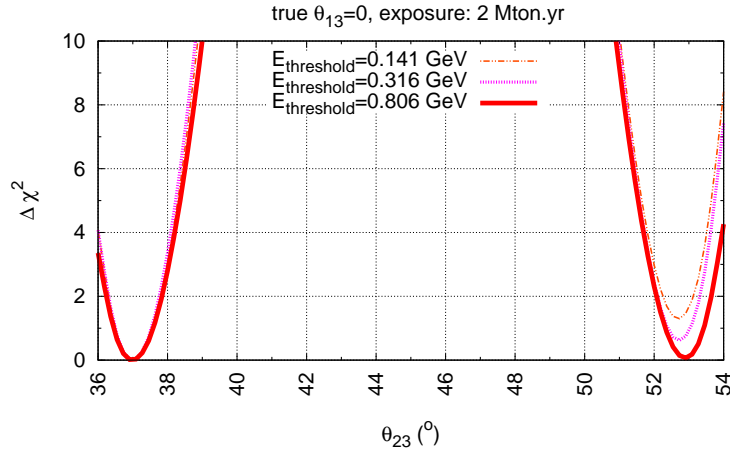


FIG. 5: The variation of  $\chi^2$  with  $\theta_{23}$  for input value of  $\theta_{23} = 37^\circ$  with threshold 0.141, 0.316, and 0.806 GeV, respectively, and  $\mathcal{E} = 2$  Mton·yr.

to  $\theta_{13} = 8.13^{+3.53}_{-7.03}^\circ$  at 95% CL [23]. New and forthcoming experiments Double Chooz, Daya Bay, RENO, T2K, NO $\nu$ A can confirm this result with higher CL or put new stringent upper bound [24] which would approximately corresponds to a situation with zero 1-3 mixing considered in the previous section.

A realistic situation would be that by the time when ICAL will collect significant statistics the angle  $\theta_{13}$  will be known with relatively good accuracy. To clarify an impact of this result on determination of the parameters of the 2-3 sector we performed an

analysis for non-zero  $\theta_{13}$ . For illustration purpose we use  $\theta_{13} = 5^\circ$  as the true value and different fit intervals with flat distribution (which could reflect errors in measurements of  $\theta_{13}$ ).

In fig. 6 we show dependence of  $\Delta^{dev} \chi^2$  defined in eq. (21) on the true (input) value of  $\theta_{23}$  for the fit value  $\theta_{23} = 45^\circ$  and  $\mathcal{E} = 1$  Mton·yr. Different curves correspond to different marginalization intervals of  $\theta_{13}$ . Comparing these results with the results of fig. 3 we find that inclusion of 1-3 mixing does not change significantly the sensitivity to the deviation

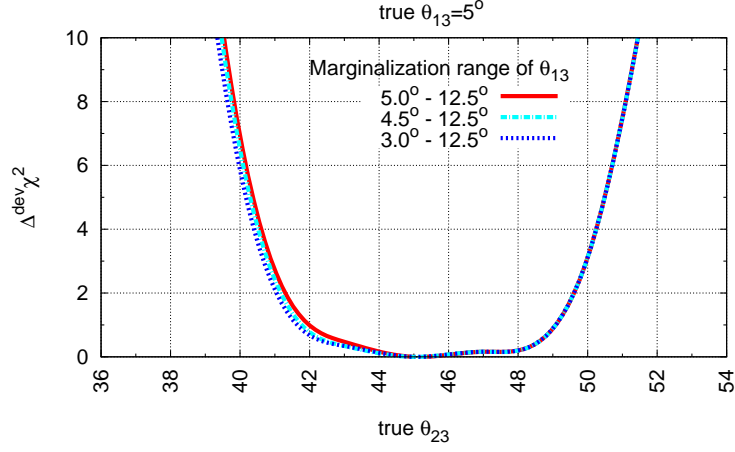


FIG. 6: The variation of the sensitivity to deviation from maximal mixing with different input values of  $\theta_{23}$  with  $\mathcal{E} = 1$  Mton-yr and threshold of 0.806 GeV. Here  $\Delta^{dev}\chi^2 = \chi^2(45^\circ) - \chi^2(\theta_{23}^{true})$ . The  $\chi^2$  is marginalized with respect to all oscillation parameters except  $\theta_{23}$ .

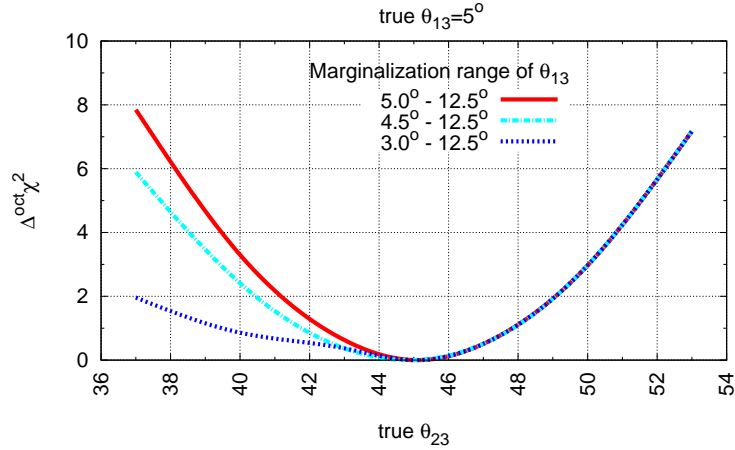


FIG. 7: The variation of the sensitivity to  $\theta_{23}$ -octant with different input values of  $\theta_{23}$  with  $\mathcal{E} = 1$  Mton-yr and threshold of 0.806 GeV. Here  $\Delta^{oct}\chi^2 = \chi^2(90^\circ - \theta_{23}) - \chi^2(\theta_{23})$ . The  $\chi^2$  is marginalized with respect to all oscillation parameters except  $\theta_{23}$ .

$\delta_{23}$ . The reason is that this sensitivity follows from the lower order effect, *i.e.*, the main mode of  $\nu_\mu$  oscillations (large probability for this mode) extends to higher energies and 1-3 mixing produces just additional distortion of the oscillatory pattern.

However, inclusion of 1-3 mixing makes the curve less symmetric with respect to  $45^\circ$  which reflects an increase of sensitivity to the octant. Also sensitivity to the deviation weakly depends on the marginalization interval for  $\theta_{13}$ .

Fig. 7 illustrates the sensitivity of ICAL to the octant in the presence of non-zero 1-3 mixing. We show dependence of  $\Delta^{oct}\chi^2$  defined in eq. (22) on true value of  $\theta_{23}$  for the fit value  $90^\circ - \theta_{23}$ . Different curves correspond to different marginalization intervals for  $\theta_{13}$ . There are two important features of the fig. 7.

The sensitivity to the octant is substantially better for non-zero value of  $\theta_{13}$  than for vanishing 1-3 mixing (fig. 7) as was also shown in previous publications. This is related to the fact that the octant



asymmetry of the flux is determined now by

$$\frac{\Delta^{oct} F}{F_\mu^0} \approx \sin 2\delta_{23} \left(1 - \frac{1}{r}\right) \langle P_A \rangle \quad (23)$$

and  $\langle P_A \rangle \sim 0.1$  in the interval  $E = (0.14 - 15)$  GeV; it is much larger than  $\langle P_S \rangle$  being enhanced in the energy range  $E = (3 - 10)$  GeV (in the resonance channel). Furthermore, at high energies  $r \sim 3 - 4$  and the value of the coefficient in eq. (23) becomes larger. As a result, for  $\theta_{23} = 51^\circ$  the octant can be identified at  $2\sigma$  level ( $\Delta^{oct} \chi^2 = 4$ ) after  $\mathcal{E} = 1$  Mton·yr, as compared with  $\Delta^{oct} \chi^2 = 0.3$  for  $\theta_{13} = 0$ .

The second feature is significant asymmetry of the curves with respect to  $\theta_{23} = 45^\circ$ . The asymmetry is practically absent for fixed input value of  $\theta_{13}$  but it increases with broadening of the marginalization interval and more importantly with increase of the power border of this interval. For  $\theta_{23} > 45^\circ$  the curves (sensitivity) is practically not changed with change of the interval, whereas for  $\theta_{23} < 45^\circ$  the sensitivity substantially decreases. E.g. for  $\theta_{23} = 40^\circ$  we obtain  $\Delta \chi^2 = 1$  for the interval  $\theta_{13} = 3^\circ - 12.5^\circ$  instead of  $\Delta^{oct} \chi^2 = 3$  for fixed value  $\theta_{13} = 5^\circ$ .

This asymmetry can be readily understood from the analytic consideration of sec. II. Neglecting the effect of 1-2 mixing the  $\nu_\mu$  flux can be presented as

$$\frac{F_\mu}{F_\mu^0} \approx K(\sin 2\theta_{23}) - f(\theta_{23}) \left(1 - \frac{1}{r}\right) P_A(\theta_{13}), \quad (24)$$

where  $K(\sin 2\theta_{23})$  is an even function of the deviation (symmetric with respect to change of the octant), and

$$f(\theta_{23}) \equiv \left(s_{23}^4 - \frac{s_{23}^2}{r}\right) \quad (25)$$

quickly increases with  $\theta_{23}$ , so that for  $r = 3 - 4$ :  $f(\theta_{23} = 40^\circ) \ll f(\theta_{23} > 50^\circ)$ . Therefore for  $\theta_{23} < 45^\circ$  the flux  $F_\mu$  has much weaker dependence on  $\theta_{13}$  than for  $\theta_{23} > 45^\circ$ . In the process of marginalization over  $\theta_{13}$  we compare true value of the flux  $F_\mu^{true}$  with the fit value  $F_\mu^{fit}$ , and  $\Delta^{oct} \chi^2$  is proportional to their difference:

$$\frac{1}{F_\mu^0} |F_\mu^{true} - F_\mu^{fit}| = \left(1 - \frac{1}{r}\right) \times |f(\theta_{23}) \langle P_A(\theta_{13}^{true}) \rangle - f(90^\circ - \theta_{23}) \langle P_A(\theta_{13}) \rangle| \quad (26)$$

If the fit value of 1-3 mixing is fixed:  $\theta_{13}^{fit} = \theta_{13}^{true}$ , the curve is approximately symmetric with respect to change  $\theta_{23} \leftrightarrow (90^\circ - \theta_{23})$ . Indeed, in this case we have from eq. (26)

$$\frac{1}{F_\mu^0} |F_\mu^{true} - F_\mu^{fit}| = \left(1 - \frac{1}{r}\right) \times \langle P_A(\theta_{13}^{true}) \rangle |f(\theta_{23}) - f(90^\circ - \theta_{23})|. \quad (27)$$

The situation is different if  $\theta_{13}$  can be varied in certain interval  $\theta_{13} = \theta_{13}^{min} - \theta_{13}^{max}$ , and we perform marginalization over  $\theta_{13}$  in this interval. Marginalization minimizes the difference of fluxes (eq. (26)) over  $\theta_{13}$  for a given value of  $\theta_{23}$ . If  $\theta_{23} < 45^\circ$ , then  $f(\theta_{23}) \ll f(90^\circ - \theta_{23})$ . In this case the difference of fluxes is minimal if  $\theta_{13} \sim \theta_{13}^{min}$ . Indeed, since  $\langle P_A \rangle$  decreases with  $\theta_{13}$ , a small value of  $\langle P_A \rangle$  partially compensates large value of  $f(90^\circ - \theta_{23})$  in the second term on the right hand side of eq. (26). Furthermore, the smaller  $\theta_{13}^{min}$  the stronger compensation is possible and therefore the smaller  $\Delta \chi^2$  can be obtained. If  $\theta_{23} > 45^\circ$ , then  $f(\theta_{23}) \gg f(90^\circ - \theta_{23})$ . Now to compensate the first term in eq. (26) one should take  $\langle P_A(\theta_{13}^{fit}) \rangle \gg \langle P_A(\theta_{13}) \rangle$ . This is, however, not possible for the considered values of  $\theta_{13}$ . Thus, in the case of unprecise determination of  $\theta_{13}$  the sensitivity to the octant is higher for  $\theta_{23} > 45^\circ$ .

### C. Determination of the 2-3 mass split. CPT test

Important advantage of a magnetized calorimeter is that it allows one to measure neutrino mass differences and mixing angles in neutrino and antineutrino channel separately. A difference of results can be related to some effective or fundamental violation of CPT symmetry.

In fig. 8 we show dependence of  $\Delta \chi^2$  on the fit values of  $\Delta m_{32}^2$  for the true value  $\Delta m_{32}^2 = -2.35 \cdot 10^{-3}$  eV<sup>2</sup> in the neutrino and antineutrino channels. We take  $\theta_{13} = 5^\circ$  and  $\theta_{23} = 45^\circ$ . According to this figure after 0.25 Mton·yr the value  $\Delta m_{32}^2 = 3.3 \cdot 10^{-3}$  eV<sup>2</sup> can be discriminated from the true value at about  $2\sigma$  level.

The accuracy of measurement of  $\Delta m_{32}^2$  is better for  $\nu$ -channel. For  $\mathcal{E} = 0.25$  Mton·yr the error in  $\nu$ -channel is about two times smaller than that in  $\bar{\nu}$  channel. The difference decreases with increase of exposure: for 1 Mton·yr it becomes about 25%. The curves  $\Delta \chi^2$  are asymmetric with respect to  $\Delta m_{32}^{2, true}$ , which is related to the dependence of oscillation probability on  $\Delta m_{32}^2$ .

The  $1\sigma$  error for  $\Delta m_{23}^2$  could be  $\pm 0.15 \cdot 10^{-3}$  eV<sup>2</sup> and  $\pm 0.04 \cdot 10^{-3}$  eV<sup>2</sup> after 0.25 Mton·yr and 1 Mton·yr exposures correspondingly. With 1 Mton·yr the first error can be achieved at  $3\sigma$  level. At 90% CL (1 Mton·yr) one can obtain  $\pm 0.08 \cdot 10^{-3}$  eV<sup>2</sup> which is better than the present MINOS result.

In figs. 9 and 10 we show  $\Delta \chi^2$  as function of  $\Delta m_{32}^2$  and  $\theta_{23}$  in neutrino and antineutrino channels for  $\mathcal{E} = 0.25$  and 1 Mton·yr. As true values we take

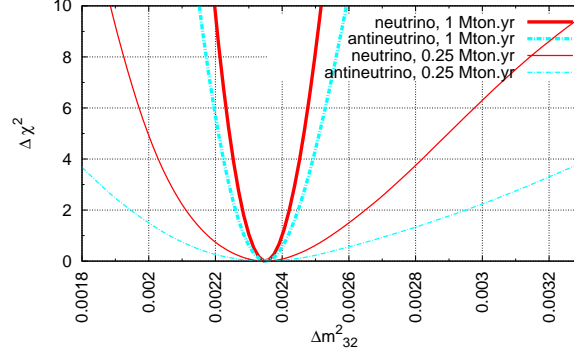


FIG. 8: The variation of  $\chi^2$  with  $\Delta m_{32}^2$  for neutrino and antineutrino with  $\mathcal{E} = 0.25$  and 1 Mton·yr with threshold 0.8 GeV. The marginalization is done over all oscillation parameters except  $\Delta m_{32}^2$ . The  $\chi^2$  values 1, 4, 9 correspond to  $1\sigma$  (68.3%),  $2\sigma$  (95.4%), and  $3\sigma$  (99.73%), respectively.

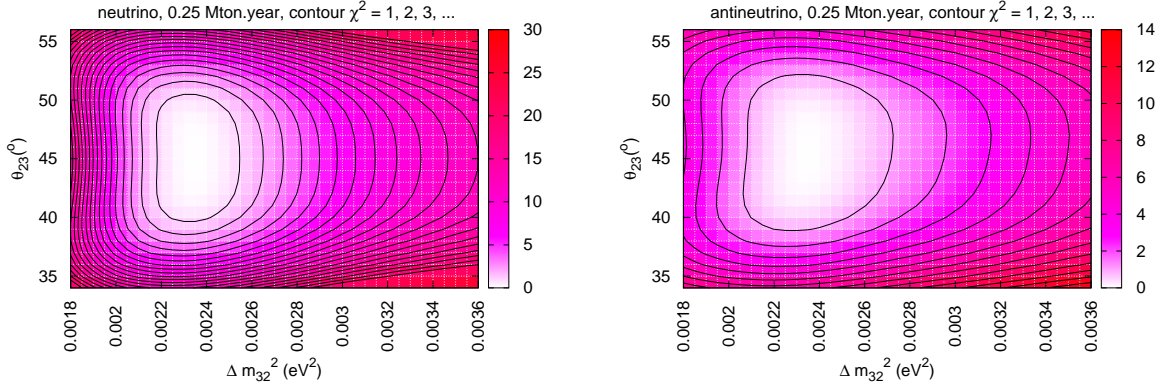


FIG. 9: The iso- $\chi^2$  contours (from inner side  $\chi^2 = 1$  with increment 1) in  $\Delta m_{32}^2 - \theta_{23}$  plane for neutrino (left) and antineutrino (right) with  $\mathcal{E} = 0.25$  Mton·yr. We set input  $\Delta m_{32}^2 = -2.35 \times 10^{-3} \text{ eV}^2$ ,  $\theta_{23} = 45^\circ$  and  $\theta_{13} = 5^\circ$  and threshold of 0.8 GeV. The  $\Delta\chi^2$  values 2.3, 4.6, 9.2 correspond to  $1\sigma$  (68.3%),  $2\sigma$  (90%), and  $3\sigma$  (99%), respectively.

$\theta_{23} = 45^\circ$  and  $\Delta m_{32}^2 = 2.35 \cdot 10^{-3} \text{ eV}^2$ . According to fig 10 the present MINOS result for  $\bar{\nu}$  ( $|\Delta m_{31}^2| = 3.36 \cdot 10^{-3} \text{ eV}^2$ ,  $\theta_{23} = 34^\circ$ ) can be excluded at about  $6\sigma$  level after  $\mathcal{E} = 1$  Mton·yr with atmospheric neutrinos.

## V. DISCUSSION AND CONCLUSION

In this paper we have presented the conservative estimations of sensitivity of ICAL to the parameters of 2-3 sector. We find that with the 1 Mton·yr exposure the  $3\sigma$  accuracy of determination of the deviation will be  $|\delta_{23}| \approx 6^\circ$ , which is better than the present global fit result and slightly better than expected sensitivity of T2K ( $\approx 9^\circ$ ). The accuracy of measurements of  $\Delta m_{23}^2$  by ICAL,  $\pm 0.15 \cdot 10^{-3} \text{ eV}^2$  ( $3\sigma$ , 1 Mton·yr exposure), is two times better than the accuracy of

the present global fit and it is worthier than expected sensitivity of T2K. ICAL, however, can provide very sensitive searches for differences of the oscillation parameters in the neutrino and antineutrino channels, *i.e.*, perform the CPT test. Can sensitivity of ICAL be further improved?

1. In our  $\chi^2$  analysis for simplicity we choose flat distributions of uncertainties of the oscillation parameters during marginalization. We can add the prior contribution of the parameters to  $\chi^2$ . This will substantially improve the sensitivity. Proper procedure would require the use of the best-fit values and possible variations of parameters (especially  $\theta_{13}$ ) which will be possible after results of forthcoming experiments will be known. This can be implemented by adding the prior contribution.

In fig. 11 and 12 we show improvements of the

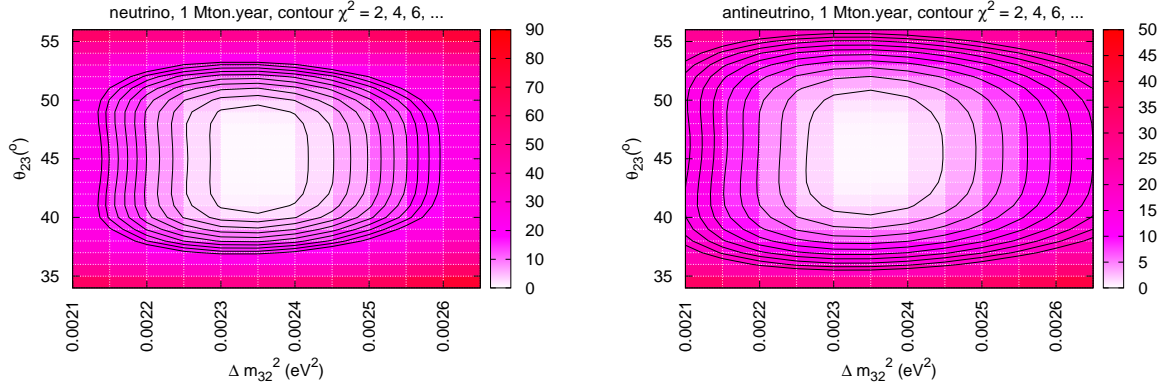


FIG. 10: The same plot (but from inner side  $\chi^2 = 2$  with increment 2) of fig. 9 with  $\mathcal{E} = 1$  Mton-yr.

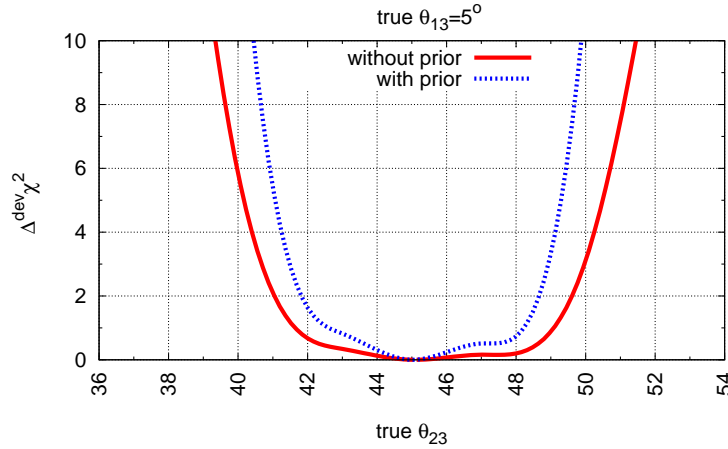


FIG. 11: The same plot of fig. 6 (variation of the sensitivity to deviation from maximal mixing with different input values of  $\theta_{23}$ ), but showing improvement due to the contribution to the  $\chi^2$  from prior knowledge of oscillation parameters. The marginalization range for  $\theta_{13}$  is  $3^\circ - 12.5^\circ$  ( $0^\circ - 12.5^\circ$ ) in absence (presence) of prior contribution.

sensitivities for the prior contribution. The asymmetry in sensitivity to octant (which was due to the uncertainty of  $\theta_{13}$  in absence of prior contribution) now disappears, and the result does not depend on marginalization range. We have assumed Gaussian distribution of the uncertainties around the best fit with width  $\sigma_{\sin^2 2\theta_{13}} = 0.01$ ,  $\sigma_{\sin^2 2\theta_{23}} = 0.015$  and  $\sigma_{\Delta m_{32}^2}/\Delta m_{32}^2 = 0.015$  following [25].

2. Can the sensitivity be improved if the flux and the cross-section uncertainties are reduced? In fig. 13 and 14 we illustrate improvement of the sensitivities with reduction of the different systematic uncertainties. If we change overall flux normalization, ratio of horizontal/vertical flux, cross-section, and tilt (below 1 GeV) uncertainties from 10%, 10%, 2%, and

15% to 2%, 2%, 2%, and 3%, respectively, we find no significant improvement of the sensitivities. Here the up-going neutrinos (far from detector) oscillates and down-going neutrinos (near to detector) almost remain unchanged. In  $\chi^2$  analysis these down-going neutrinos act to reduce the effect of systematic uncertainties. A significant improvement occurs only when all systematic uncertainties are zero.

3. Measurements of the hadron energy in ICAL in addition to the muon energy is expected to improve substantially reconstruction of the neutrino energy for  $E \gtrsim 2$  GeV. However, the energy resolution for hadron is roughly 80% and number of hits (number of active detector layers in which signal is detected) increases only logarithmically with  $E$ . The

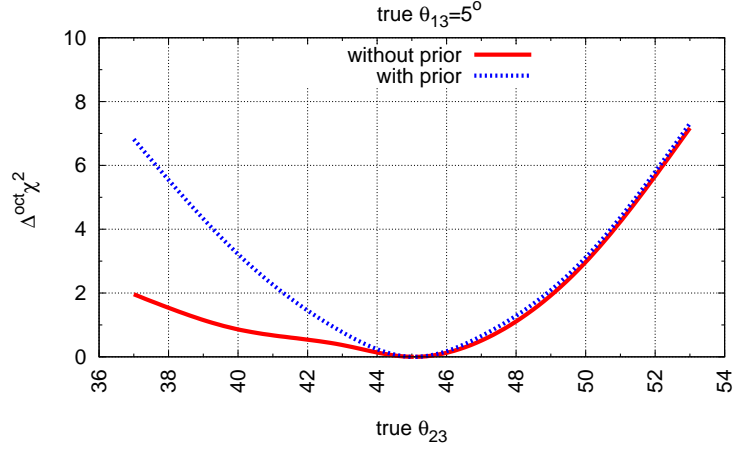


FIG. 12: The same plot of fig. 7 (variation of the sensitivity to  $\theta_{23}$ -octant with different input values of  $\theta_{23}$ ), but showing improvement due to the contribution to the  $\chi^2$  from prior knowledge of oscillation parameters. The marginalization range for  $\theta_{13}$  is  $3^\circ - 12.5^\circ$  ( $0^\circ - 12.5^\circ$ ) in absence (presence) of prior contribution.

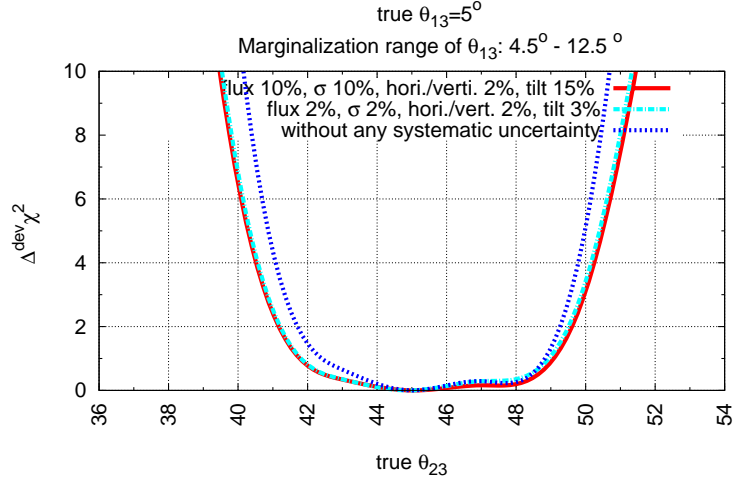


FIG. 13: The same plot of fig. 6 (variation of the sensitivity to deviation from maximal mixing with different input values of  $\theta_{23}$ ), but showing the improvement with reduction of systematic uncertainties.

realistic estimation of this improvement can be done only in GEANT-based studies. Moreover, in contrast to muons the number of hits produced by the hadron shower strongly depends on the thickness of iron layers.

4. Larger values of  $\theta_{13}$  can substantially enhance the sensitivity to the octant since  $P_A \sim \sin^2 \theta_{13}$  at low energies.

In conclusion, we have studied analytically the dependence of the  $\theta_{23}$ -deviation effect and the octant asymmetry of  $\nu_\mu$  and  $\bar{\nu}_\mu$  fluxes on the neutrino pa-

rameters  $\theta_{23}$  and  $\theta_{13}$ . We explored the sensitivity of magnetized calorimeter to the  $\theta_{23}$ -deviation and octant as well as to  $\Delta m_{32}^2$ .

We show that for  $\theta_{13} = 0$  the sensitivity of ICAL to the octant is low even for maximally allowed values of deviation of the 2-3 mixing from maximal. This is related to the fact that the octant asymmetry is proportional to the “solar” probability  $P_S$  which is  $O(1)$  at  $E \sim 0.1$  GeV but quickly, as  $\propto E^{-2}$ , decreases with energy. The situation can be improved by lowering the threshold, increasing exposure and reducing

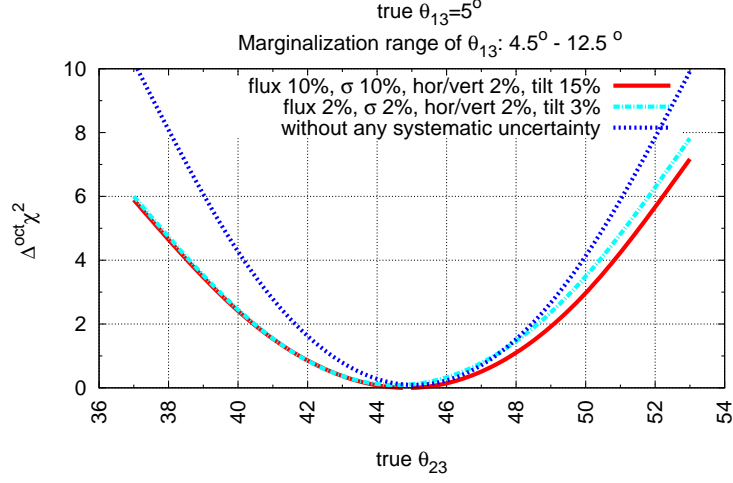


FIG. 14: The same plot of fig. 7 (variation of the sensitivity to  $\theta_{23}$ -octant with different input values of  $\theta_{23}$ ), but showing the improvement with reduction of systematic uncertainties.

TABLE I: Results of determination of  $\theta_{23}$

$\theta_{23}$	CL	Source
$42.9^{+4.1}_{-2.8}^\circ$	$1\sigma$	global-fit[2]
$35.7^\circ - 54^\circ$	$3\sigma$	global-fit[2]
$45^{+10}_{-7.8}^\circ$	99%	SK [4]
$45^\circ \pm 9^\circ$	90%	MINOS ( $\nu$ ) [4]
$34^{+6}_{-4}^\circ$ or $56^{+4}_{-6}^\circ$	90%	MINOS ( $\bar{\nu}$ ) [5]
$39^\circ - 51^\circ$	$2\sigma$	T2K [7]
$36^\circ - 54^\circ$	$2\sigma$	NO $\nu$ A [7]
$40^\circ - 50^\circ$	$2\sigma$	INO (1 Mton-yr)

TABLE II: Results of determination of  $\Delta m_{31}^2$

$\Delta m_{32}^2 (10^{-3} \text{eV}^2)$	CL	Source
$-2.36 \pm 0.07 (\pm 0.36)$	$1 (3)\sigma$	global-fit [2]
$+2.47 \pm 0.12 (\pm 0.37)$	$1 (3)\sigma$	global-fit [2]
$2.5^{+0.52}_{-0.60}$	99%	SK $3\nu$ [4]
$2.35^{+0.11}_{-0.08}$	90%	MINOS $\nu$ [5]
$3.36^{+0.45}_{-0.40}$	90%	MINOS $\bar{\nu}$ [5]
$2.5 \pm 0.04$	$2\sigma$	T2K [7]
$2.5^{+0.07}_{-0.04}$	$2\sigma$	NO $\nu$ A [7]
$2.5 \pm 0.09$	$2\sigma$	INO (1 Mton-yr)

systematic errors (especially in spectral index). We find that the  $sign(\delta_{23})$  can be established at 90% CL if  $|\delta_{23}| = 7^\circ$ ,  $\mathcal{E} = 4$  Mton-yr and threshold of 0.141 GeV.

ICAL has good sensitivity to the  $\theta_{23}$ -deviation from maximal 2-3 mixing: the effect is proportional to the probability of the main channel oscillation  $\nu_\mu - \nu_\tau$  which is unsuppressed in whole considered neutrino energy range. As a result, dependence of sensitivity on threshold is weak and it does not change substantially when the effect of 1-3 mixing is included.

Oscillations driven by non-zero 1-3 mixing substantially improve the sensitivity to the octant. One can determine the  $sign(\delta_{23})$  for  $\delta_{23} = 5^\circ$  and  $\theta_{13} = 5^\circ$

at 90% CL after 1 Mton-yr exposure.

We find that this sensitivity depends crucially on the uncertainty range of  $\theta_{13}$  value. For a given nonzero  $\theta_{13}$ , the sensitivity to octant discrimination is symmetric in  $\theta_{23}$  with respect to  $\theta_{23} = 45^\circ$ . However, the asymmetry arises (smaller sensitivity for  $\theta_{23} < 45^\circ$ ) if value of  $\theta_{13}$  can vary in some range. The symmetry is restored if prior for 1-3 mixing is added.

ICAL can measure the difference of  $\Delta m_{32}^2$  in  $\nu$  and  $\bar{\nu}$  channels (CPT test) with accuracy  $0.8 \times 10^{-4} \text{eV}^2$  at  $3\sigma$  confidence level with 1 Mton-yr exposure and the present MINOS result can be excluded at  $> 5\sigma$  confidence level.

*Acknowledgments:* The use of general cluster facility of Harish-Chandra Research Institute for a part

of this work is gratefully acknowledged.

- 
- [1] R. N. Mohapatra and A. Y. Smirnov, *Ann. Rev. Nucl. Part. Sci.* **56**, 569 (2006) [arXiv:hep-ph/0603118]; and the reference there in.
  - [2] M. C. Gonzalez-Garcia, M. Maltoni and J. Salvado, *JHEP* **1004**, 056 (2010) [arXiv:1001.4524 [hep-ph]].
  - [3] G. L. Fogli, E. Lisi, A. Marrone, A. Palazzo and A. M. Rotunno, *Phys. Rev. Lett.* **101**, 141801 (2008) [arXiv:0806.2649 [hep-ph]].
  - [4] J. Hosaka *et al.* [Super-Kamiokande Collaboration], *Phys. Rev. D* **74**, 032002 (2006) [arXiv:hep-ex/0604011].
  - [5] P. Vahle [MINOS Coll.] (2010), Presentation at International conference ‘Neutrino 2010’ in Athens, Greece. See slides at <http://www.neutrino2010.gr/>.
  - [6] J. Kopp, P. A. N. Machado and S. J. Parke, arXiv:1009.0014 [hep-ph].
  - [7] P. Huber, M. Lindner, M. Rolinec, T. Schwetz and W. Winter, *Nucl. Phys. Proc. Suppl.* **145**, 190 (2005) [arXiv:hep-ph/0412133].
  - [8] C. W. Kim and U. W. Lee, *Phys. Lett. B* **444**, 204 (1998) [arXiv:hep-ph/9809491].
  - [9] O. L. G. Peres and A. Y. Smirnov, *Nucl. Phys. B* **680**, 479 (2004) [arXiv:hep-ph/0309312].
  - [10] O. L. G. Peres and A. Y. Smirnov, *Phys. Rev. D* **79**, 113002 (2009) [arXiv:0903.5323 [hep-ph]].
  - [11] M. C. Gonzalez-Garcia, M. Maltoni and A. Y. Smirnov, *Phys. Rev. D* **70**, 093005 (2004) [arXiv:hep-ph/0408170].
  - [12] S. Choubey and P. Roy, *Phys. Rev. D* **73**, 013006 (2006) [arXiv:hep-ph/0509197].
  - [13] D. Indumathi, M. V. N. Murthy, G. Rajasekaran and N. Sinha, *Phys. Rev. D* **74**, 053004 (2006) [arXiv:hep-ph/0603264].
  - [14] A. Bandyopadhyay *et al.* [ISS Physics Working Group], *Rept. Prog. Phys.* **72**, 106201 (2009) [arXiv:0710.4947 [hep-ph]].
  - [15] A. Samanta, *Phys. Rev. D* **80**, 113003 (2009) [arXiv:0812.4639 [hep-ph]].
  - [16] E. K. Akhmedov, M. Maltoni and A. Y. Smirnov, *JHEP* **0806**, 072 (2008) [arXiv:0804.1466 [hep-ph]].
  - [17] A. M. Dziewonski and D. L. Anderson, *Phys. Earth Planet. Interiors* **25**, 297 (1981).
  - [18] D. Casper, *Nucl. Phys. Proc. Suppl.* **112**, 161 (2002) [arXiv:hep-ph/0208030].
  - [19] <http://geant4.web.cern.ch/geant4/>
  - [20] A. Samanta, *Phys. Rev. D* **79**, 053011 (2009) [arXiv:0812.4640 [hep-ph]].
  - [21] M. Honda, T. Kajita, K. Kasahara, S. Midorikawa and T. Sanuki, *Phys. Rev. D* **75**, 043006 (2007) [arXiv:astro-ph/0611418].
  - [22] A. Samanta, *Phys. Rev. D* **81**, 037302 (2010) [arXiv:0907.3540 [hep-ph]].
  - [23] B. Aharmim *et al.* [SNO Collaboration], *Phys. Rev. C* **81**, 055504 (2010) [arXiv:0910.2984 [nucl-ex]].
  - [24] M. Mezzetto and T. Schwetz, *J. Phys. G* **37**, 103001 (2010) [arXiv:1003.5800 [hep-ph]].
  - [25] P. Huber, M. Lindner, M. Rolinec, T. Schwetz and W. Winter, *Phys. Rev. D* **70**, 073014 (2004) [arXiv:hep-ph/0403068].